communities, values of $b_{i,j}$ were selected from uniform distributions between 0 and −0.1 (plant–plant competition), −0.3 (herbivores → plants; that is, the effect of herbivores on plants), 0.1 (plants → herbivores), −0.1 (predators → herbivores), and 0.05 (herbivores → predators). Intraspecific interactions were selected at random between −0.1 and −0.2 for plants, and set to −0.2 for herbivores and predators. For competitive communities, interspecific values of $b_{i,j}$ were selected uniformly between 0 and −0.1, and intraspecific values between −0.06 and −0.16. For the arbitrary topology, the probability of any pair of species interacting was 0.5, and of the interacting pairs of species 45% were competitors, 45% were prey and predators, and 10% were mutualists. The magnitudes of interspecific values of $b_{i,j}$ were selected uniformly between 0 and 0.1, with sign dictated by type of interaction, and intraspecific values were selected between −0.06 and −0.16.

For the random food webs (Fig. 3), we selected intra- and interspecific values of $b_{i,j}$ from uniform (−0.1, 0) and (−0.1, 0.1) distributions, respectively. The interaction coefficients $b_{i,j}$ were then modified by multiplying interspecific coefficients by p. The vast majority of resulting food webs when $p > 0.5$ were unstable, but comparable analyses constrained to stable food webs gave similar results.

In selecting coefficients, we constrained values for intraspecific interactions $b_{i,i}$ to negative numbers. Otherwise, for the case of no interactions (or when communities are reduced to one species) intensifying the stressor increases species abundances. This is because in the absence of species interactions, $\delta_i(N) = -a_i/b_{i,i}$, which is positive when $b_{i,i} > 0$.

Values of $\delta_i(N)$ were calculated by solving the set of equations satisfied by equation (1) at equilibrium:

$$r_i + a_i s + \sum_j b_{i,j} x_j^*(s) = 0 \quad (i = 1, \ldots, N) \qquad (3)$$

and new values of $\delta_i(N)$ were calculated sequentially as the community size was reduced. Our assumption that the species with the lowest tolerance $\delta_i(N)$ goes extinct first was supported by simulating the full model given by equation (2) (for example, Fig. 1a, b) and categorizing species as extinct once they were reduced in abundance by a factor of 10^{-3}.

1. Sala, O. E. et al. Global biodiversity scenarios for the year 2100. Science 287, 1170–1174 (2000).
2. Chapin, F. S. I. et al. Consequences of changing biodiversity. Nature 405, 234–242 (2000).
3. Ehrlich, P. & Ehrlich, A. Extinction (Random House, New York, 1981).
4. Terborgh, J. et al. Ecological meltdown in predator-free forest fragments. Science 294, 1923–1926 (2001).
5. Naeem, S., Thompson, L. J., Lawler, S. P., Lawton, J. H. & Woodfin, R. M. Declining biodiversity can alter the performance of ecosystems. Nature 368, 734–737 (1994).
6. Naeem, S. Ecology—Power behind diversity's throne. Nature 401, 653–654 (1999).
7. Tilman, D. et al. Diversity and productivity in a long-term grassland experiment. Science 294, 843–845 (2001).
8. Hector, A. et al. Plant diversity and productivity experiments in European grasslands. Science 286, 1123–1127 (1999).
9. Vitousek, P. M., Mooney, H. A., Lubchenco, J. & Melillo, J. M. Human domination of the Earth's ecosystems. Science 277, 494–499 (1997).
10. Davis, A. J., Jenkinson, L. S., Lawton, J. H., Shorrocks, B. & Wood, S. Making mistakes when predicting shifts in species range in response to global warming. Nature 391, 783–786 (1998).
11. Ives, A. R. Predicting the response of populations to environmental change. Ecology 76, 926–941 (1995).
12. Case, T. J. & Bender, E. A. Testing for higher order interactions. Am. Nat. 118, 920–929 (1981).
13. Yodzis, P. Introduction to Theoretical Ecology (Harper & Row, New York, 1989).
14. Frost, T. M., Carpenter, S. R., Ives, A. R. & Kratz, T. K. in Linking Species and Ecosystems (eds Jones, C. G. & Lawton, J. H.) 224–239 (Chapman and Hall, New York, 1995).
15. Ives, A. R., Carpenter, S. R. & Dennis, B. Community interaction webs and the response of a zooplankton community to experimental manipulations of planktivory. Ecology 80, 1405–1421 (1999).
16. McGrady-Steed, J. & Morin, P. J. Biodiversity, density compensation, and the dynamics of populations and functional groups. Ecology 81, 361–373 (2000).
17. Tilman, D. Biodiversity: Population versus ecosystem stability. Ecology 77, 350–363 (1996).
18. Ostfeld, R. S. & LoGiudice, K. Community disassembly, biodiversity loss, and the erosion of an ecosystem function. Ecology 84, 1421–1427 (2003).
19. Pimm, S. L., Jones, H. L. & Diamond, J. On the risk of extinction. Am. Nat. 132, 757–785 (1988).
20. MacArthur, R. H. Geographical Ecology (Harper and Row, New York, 1972).
21. Smith, M. D. & Knapp, A. K. Dominant species maintain ecosystem function with non-random species loss. Ecol. Lett. 6, 509–517 (2003).
22. May, R. M. Stability and Complexity in Model Ecosystems 2nd edn (Princeton Univ. Press, Princeton, New Jersey, 1974).
23. Pimm, S. L. Food Webs (Chapman and Hall, London, 1982).
24. Tilman, D., Wedin, D. & Knops, J. Productivity and sustainability influenced by biodiversity in grassland ecosystems. Nature 379, 718–720 (1996).
25. Peres, C. A. & Dolman, P. M. Density compensation in neotropical primate communities: evidence from 56 hunted and nonhunted Amazonian forests of varying productivity. Oecologia 122, 175–189 (2000).
26. Klug, J. L., Fischer, J. M., Ives, A. R. & Dennis, B. Compensatory dynamics in planktonic community responses to pH perturbations. Ecology 81, 387–398 (2000).
27. Paine, R. T. Food web complexity and species diversity. Am. Nat. 100, 65–75 (1966).
28. Diaz, S., Symstad, A. J., Chapin, F. S., Wardle, D. A. & Huenneke, L. F. Functional diversity revealed by removal experiments. Trends Ecol. Evol. 18, 140–146 (2003).
29. Wootton, J. T. Prediction in complex communities: Analysis of empirically derived Markov models. Ecology 82, 580–598 (2001).
30. Laska, M. S. & Wootton, J. T. Theoretical concepts and empirical approaches to measuring interaction strength. Ecology 79, 461–476 (1998).

....

Resonance effects indicate a radical-pair mechanism for avian magnetic compass

Thorsten Ritz[1], **Peter Thalau**[2], **John B. Phillips**[3], **Roswitha Wiltschko**[2] **& Wolfgang Wiltschko**[2]

[1]Department of Physics and Astronomy, University of California, Irvine, California 92697-4575, USA
[2]Zoologisches Institut, Fachbereich Biologie und Informatik, J.W. Goethe-Universität, Siesmayerstrasse 70, D-60054 Frankfurt am Main, Germany
[3]Department of Biology, 2119 Derring Hall, Virginia Tech, Blacksburg, Virginia 24061, USA

Migratory birds are known to use the geomagnetic field as a source of compass information[1,2]**. There are two competing hypotheses for the primary process underlying the avian magnetic compass, one involving magnetite**[3–5]**, the other a magnetically sensitive chemical reaction**[6–8]**. Here we show that oscillating magnetic fields disrupt the magnetic orientation behaviour of migratory birds. Robins were disoriented when exposed to a vertically aligned broadband (0.1–10 MHz) or a single-frequency (7-MHz) field in addition to the geomagnetic field. Moreover, in the 7-MHz oscillating field, this effect depended on the angle between the oscillating and the geomagnetic fields. The birds exhibited seasonally appropriate migratory orientation when the oscillating field was parallel to the geomagnetic field, but were disoriented when it was presented at a 24° or 48° angle. These results are consistent with a resonance effect on singlet–triplet transitions and suggest a magnetic compass based on a radical-pair mechanism**[7,8]**.**

The magnetic compass of birds is light-dependent[9,10], and exhibits strong lateralization with input coming primarily from the right eye[11]. However, the primary biophysical process underlying this compass remains unexplained. Magnetite[3–5,12] as well as biochemical radical-pair reactions[7,8] have been hypothesized to mediate sensitivity to Earth-strength magnetic fields through fundamentally different physical mechanisms. In the magnetite-based mechanism, magnetic fields exert mechanical forces[3]. In the radical-pair mechanism, the magnetic field alters the dynamics of transitions between spin states, after the creation of a radical pair through a light-induced electron transfer. These transitions in turn affect reaction rates and products[7,8]. Although in most radical-pair reactions the effects of Earth-strength magnetic fields are masked by stochastic fluctuations, model calculations[13] show that such effects can be amplified beyond the level of stochastic fluctuations in specialized radical-pair receptor systems.

Exploiting the principles of magnetic resonance, we developed a diagnostic tool to identify a radical-pair process as the primary process for a physiological magnetic compass. No change in magnetic alignment of magnetite receptors is expected for weak oscillating fields with frequencies larger than 100 kHz (ref. 14).
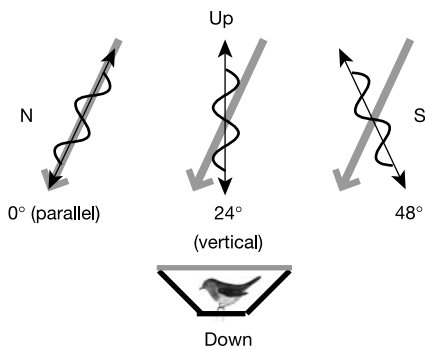
Figure 1 Experimental set-up. Orientation of the 7.0-MHz oscillating magnetic fields (black arrows with sine curve) parallel, at a 24° (vertical) and at a 48° angle to the geomagnetic field (grey arrows; see Fig. 2c–e for results). In the parallel and 48° conditions, the oscillating fields have the same angle with respect to the birds in our experimental set-up.

However, an oscillating magnetic field that is in resonance with the splitting between radical-pair spin states can perturb a radical-pair mechanism by directly driving singlet–triplet transitions. In typical biomolecules, many hyperfine splittings occur in the range of 0.1–10 MHz and a limited number may exist in the range of 10–25 MHz (ref. 15).

We used the migratory orientation of European robins, *Erithacus rubecula*, to detect the possible effects of oscillating magnetic fields on the underlying magnetoreception mechanism. Orientation tests were performed during spring migration under 565 nm light; conditions under which robins normally show excellent orientation using their inclination compass[16,17]. All birds were tested indoors, in the local geomagnetic field of 46 μT and 66° inclination. In addition to the control condition (geomagnetic field alone, no oscillating field), we used four experimental conditions in which an oscillating magnetic field was added to the geomagnetic field (Fig. 1).

In the control condition, the robins exhibited seasonally appropriate northerly orientation (Fig. 2a), but in the presence of broadband (0.1–10 MHz, 0.085 μT) and single-frequency (7 MHz, 0.47 μT) oscillating fields, both vertically aligned (see Fig. 1), the birds were disoriented (Fig. 2b, d).

To confirm that the observed behavioural change was caused by a direct effect of the oscillating fields on the magnetic compass and not by nonspecific effects due to changes in motivation and so on, we varied the alignment of the 7.0-MHz field. The frequencies at which an oscillating field perturbs a radical-pair reaction depend not only on the chemical nature of the radical pair, but also on the alignment of the oscillating field with respect to the static field[18]. This implies that the responses of a magnetic compass system based on radical pairs in the presence of a weak, single-frequency oscillating field can depend on the alignment of the oscillating field, whereas nonspecific effects should occur independently of alignment. We tilted the oscillating field 24° to the north or 24° to the south, so that the two oscillating fields were aligned at the same angle relative to the vertical, but at different angles, parallel and 48°, relative to the geomagnetic field (Fig. 1).

When the oscillating field was parallel to the geomagnetic field, the birds oriented in the migratory direction (Fig. 2c) and their response was indistinguishable from that of the control condition (Table 1). In contrast, when the same oscillating field was presented at 24° and 48° relative to the geomagnetic field, the birds were disoriented (Fig. 2d, e) and their response differed significantly from that of the control condition ($P < 0.01$). The intra-individual scatter in the distribution of nightly headings, as reflected by the length of the birds' mean vectors (r_b), was indistinguishable from that of the control condition when the 7-MHz oscillating field was parallel to the geomagnetic field, but was significantly greater (lower
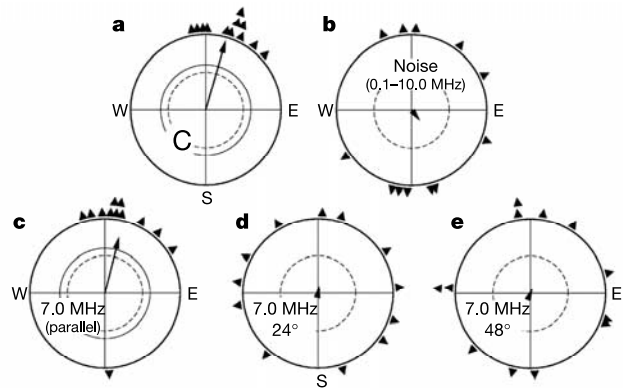
Figure 2 Effects of oscillating magnetic fields on magnetic orientation behaviour of European robins. Triangles indicate the mean headings of the 12 test birds, arrows represent the grand mean vectors (unit length = outer circle radius; see Table 1 for numerical values). The inner circles mark the 5% (dotted) and the 1% significance border of the Rayleigh test[27]. **a**, Tests in the geomagnetic field only. **b**, Tests in the geomagnetic field and a broadband (0.1–10 MHz) noise field of 0.085 μT. **c–e**, Tests in a 7.0-MHz field of 0.47 μT, oriented either parallel (**c**), at a 24° angle (**d**), or at a 48° angle (**e**) to the geomagnetic field.

r_b) in the other three oscillating-field conditions (that is, broadband and 7 MHz at 24° and 48° angles) (see Table 1).

Our findings show that it is unlikely that oscillating fields have an effect on magnetite-based receptors[3–5,12], because the dampening effects of the cellular environment prevent magnetite particles from tracking weak radio-frequency magnetic fields. Even in very-low-viscosity physiological conditions (spherical single-domain magnetite in water) we can estimate, following ref. 14, that a 7-MHz field would require an intensity of 285 μT to produce a noticeable change in alignment, which is far stronger than the 0.47 μT fields used in our experiments. Likewise, frequencies used in these experiments of less than 10 MHz are far from the expected ferromagnetic resonance frequencies in the GHz range[19], thus rendering thermal or lattice vibration effects of the oscillating fields on magnetite unlikely.

In contrast, resonance effects of oscillating magnetic fields in the frequency range of 0.1–10 MHz are expected in a radical-pair mechanism because hyperfine splittings occur in this range[15]. Resonance effects in this frequency range would also be expected in the context of Leask's optical pumping hypothesis[6], although the lack of evidence for a biological source of energy in the radio-frequency range required by the optical-pumping process[6] makes this mechanism unlikely.

By what physical mechanism could the remarkably weak oscillating fields used in our experiments (0.085 μT, 0.47 μT) affect a radical-pair reaction, and in turn, a radical-pair-based compass system? A simple model calculation (see Methods) suggests that at least in some radical-pair reactions (radical pairs with one dominant hyperfine interaction and a long lifetime), a resonant oscillating magnetic field of a thousandth of the geomagnetic field strength can produce a detectable effect. This remarkable sensitivity to very weak resonant oscillating fields is a noteworthy feature and further studies should analyse the limits of sensitivity in more realistic descriptions of radical pairs.

Our data, together with the above analysis, indicate that a magnetically sensitive radical-pair process in European robins is linked to the physiology of magnetic compass orientation. The most straightforward explanation for our findings is that the radical-pair process indicated by our experiments works as the primary process underlying magnetic compass orientation in European robins and probably in other birds[10]. Of course, we cannot exclude the possibility that a radical-pair reaction that is part of an unrelated biochemical pathway was affected. However, the fact that resonance

Table 1 **Orientation of European robins in different oscillating magnetic field conditions**

Bird	Geomagnetic field only		Noise (0.1–10 MHz)		7.0 MHz parallel		7.0 MHz 24°		7.0 MHz 48°	
	α_b	r_b	α_b	r_b	α_b	r_b	α_b	r_b	α_b	r_b
R 1	26°	0.98	339°	0.24	358°	1.00	110°	0.53	274°	0.45
R 2	20°	0.76	183°	0.42	4°	0.95	126°	0.48	9°	0.84
R 3	47°	0.91	194°	0.61	344°	0.70	86°	0.32	226°	0.98
R 4	350°	0.72	3°	0.21	10°	0.99	17°	0.37	32°	0.20
R 5	15°	0.94	189°	0.74	12°	0.99	162°	0.37	112°	0.85
R 6	1°	0.94	37°	0.90	27°	0.80	330°	0.29	351°	0.17
R 7	18°	1.00	64°	0.42	350°	0.29	297°	0.44	193°	0.73
R 8	20°	0.99	112°	0.51	57°	0.45	220°	0.96	109°	0.11
R 9	354°	0.97	354°	0.80	177°	0.27	58°	0.89	177°	0.32
R 10	24°	0.82	166°	0.09	8°	0.99	261°	0.42	352°	0.15
R 11	358°	0.81	163°	0.84	6°	0.99	278°	0.28	75°	0.80
R 12	37°	0.79	235°	0.47	41°	0.86	3°	0.78	273°	0.31
Grand mean vector	16°, 0.96***		142°, 0.18[n.s.]		14°, 0.78***		11°, 0.10[n.s]		22°, 0.07[n.s.]	
Median individual vector length	0.93		0.49		0.90		0.43		0.38	
ΔC	C	C	**	***	n.s.	n.s.	**	***	**	**

The α_b and r_b values are based on three recordings of the bird under the respective condition. The grand mean vector is given with its significance by the Rayleigh test indicated by asterisks, followed by the median individual vector length. The bottom line indicates significant differences from the control data obtained in the geomagnetic field only (see Methods for tests). Significance levels: ***, $P < 0.001$; **, $P < 0.01$; n.s., not significant.

effects are only expected in specialized radical-pair systems that can also detect the geomagnetic field[7,13], makes it unlikely that a radical-pair process not associated with magnetoreception was affected. There is currently no evidence supporting the existence of such a magneto-sensitive radical-pair process outside the context of magnetoreception and even if one existed, it is uncertain whether it would affect orientation behaviour. In our study we observed no change in activity between birds in oscillating-field and control conditions; and food intake and the general appearance of the birds was normal, suggesting that their health and motivation were unaffected by the brief 75 min exposure to oscillating magnetic fields. In view of this, our findings probably reflect a direct effect of the oscillating fields on the compass mechanism.

This conclusion does not rule out the possibility that birds possess an additional magnetically sensitive system based on magnetite. Magnetite in the form of single domains and super-para-magnetic crystals embedded in specialized structures has been described in the ethmoid region and in the upper beak of migratory birds and pigeons[20,21]. However, behavioural evidence[22–24] as well as electrophysiological recordings[25,26] suggest that the magnetite discovered is not involved in magnetic compass orientation, but instead forms the basis of a magnetic-intensity sensor, potentially used in a magnetic 'map' sense for determining geographic position.

Our study establishes the use of oscillating magnetic fields as a diagnostic tool that can indicate the involvement of a magneto-sensitive radical-pair reaction in birds. Extending this tool to determine the frequency range in which oscillating fields affect the radical-pair mechanism can reveal the chemical nature of the radical pairs involved. Finally, using oscillating magnetic fields as a diagnostic tool is not specific to birds and should be easily transferable to assays with other animal groups. The threshold intensity at which oscillating-field effects can be observed provides information about the underlying mechanism. Behavioural effects from oscillating fields of similar intensity to those used in the present study would suggest a radical-pair mechanism. The absence of behavioural effects from oscillating fields of intensities greater than 50 µT would make a radical-pair mechanism unlikely. □

Methods

Test birds

European robins are small passerines that migrate at night. The test birds were mist-netted as transmigrants in early September 2002 in the Botanical Garden near the Zoological

Institute in Frankfurt am Main (50° 08′ N, 8° 40′ E). The birds were kept indoors in individual cages over the winter on a photoperiod that simulated local conditions until December, but was then reduced to 8:16 h light:dark. In the beginning of January 2003, the photoperiod was increased to 13:11 h light:dark. This induced premature *Zugunruhe* (nocturnal migratory restlessness); the experiments took place between 13 January and 17 February 2003.

Test conditions

The tests took place in wooden huts in the garden of the Zoological Institute within the local geomagnetic field of 46 µT and 66° inclination. To produce the oscillating fields, we modified a test design developed by J.B.P. for similar tests (J.B.P., unpublished), consisting of a coil antenna (210 cm diameter) mounted on a rotatable wooden frame surrounding the test arena. Oscillating currents from a high frequency (HF) generator (Stanford Research Systems DS 34) were amplified by a HF amplifier (Research AF Model 25 W 1,000) and fed into the coil through a resistance of 51 Ω. The coil consisted of a single winding of coaxial cable (RG62A/U, 93 Ω) with 2 cm of the screening removed opposite the feed. The HF field was measured daily, before each test session, using a spectrum analyser (HP89410A) and a magnetic field probe (Rohde & Schwarz, HZ-11816.2770.0, 3 cm probe). Within the test arena, the inhomogeneity of the field was less than 15%. Variations in field intensities between tests were less than 20% of the average value. The HF generator and amplifier were placed outside the huts in varying positions with respect to the test arena. They were switched on during the majority of control tests, but with the power generator turned to zero; comparisons with control tests without this arrangement revealed no observable effect of this procedure.

Test apparatus and procedure

Testing followed standard procedures[16]: birds were tested individually in funnel-shaped PVC cages (35 cm upper diameter; 20 cm high) lined with coated paper (BIC Germany, formerly TippEx); the birds left scratches in the coating as they moved. The cages were covered with an opaque plexiglass cover and placed in PVC cylinders, the top of which consisted of a plastic disk carrying the same green light-emitting diodes as those used in earlier studies[9,16] (peak frequency at wavelength $\lambda = 565$ nm, with $\lambda/2$ at 533 and 583 nm, respectively). The light passed through two diffusers before reaching the bird with an intensity of 2.1 mW m^{-2}.

The birds were tested once per day. Tests began when the light went out in the housing cages and lasted about 75 min. Each bird was tested three times in each condition. The three tests were arranged in sets; the set of second and third tests began after the set of first and second tests respectively was completed. Within each set, the tests in the various conditions were performed in a pseudo-random order, with the sequence differing between birds.

Data analysis and statistics

For the data analysis, the coated paper was divided into 24 sectors, and the scratches per sector were counted by experimenters that were blind to the test condition. The heading of the respective test was determined by vector addition. From the three headings per test condition for each bird, the mean vector with heading α_b, and length r_b, was calculated. The twelve α_b values were combined to a grand mean vector, which was tested for directional significance using the Rayleigh test[27]. The distributions of the birds' α_b values in different conditions were compared using the Mardia–Watson–Wheeler test[27]. The r_b values, representing the intra-individual variance in locating the migratory direction, are not normally distributed; and so medians are given for each test condition. The r_b values were compared with those obtained under the control conditions using the Wilcoxon test for matched pairs of data.

letters to nature

Model calculations

We used a one-proton radical-pair model[28] with an isotropic hyperfine coupling, a, of 0.5 mT, an anisotropy, α of 0.3, and a lifetime of 20 µs (corresponding to the observed lifetime of flavin-tryptophan radical pairs[15]). We solved the stochastic Liouville equation to determine the triplet yield in the presence of a static magnetic field of 46 µT. We then calculated, by direct numerical integration of the stochastic Liouville equation, the change in triplet yield, $\Delta\Phi_{OMF}$, caused by an additional 1.3 MHz oscillating magnetic field in resonance with the splitting due to the 46 µT static field. For comparison, we also calculated the triplet yield change, $\Delta\Phi_{static}$, resulting from a decrease of 12 µT in static field, noting that such a change led to disorientation in the magnetic compass orientation responses of robins[29]. The intensity of the oscillating field required for $\Delta\Phi_{OMF}$ to equal $\Delta\Phi_{static}$ is 0.033 µT, that is, less than any of the intensities employed in our experiments.

1. Wiltschko, W. & Wiltschko, R. Magnetic compass of European robins. Science 176, 62–64 (1972).
2. Wiltschko, R. & Wiltschko, W. Magnetic Orientation in Animals (Springer, Berlin, 1995).
3. Kirschvink, J. & Gould, J. Biogenic magnetite as a basis for magnetic field detection in animals. BioSystems 13, 181–201 (1981).
4. Edmonds, D. T. A sensitive optically detected magnetic compass for animals. Proc. R. Soc. Lond. B 263, 295–298 (1996).
5. Shcherbakov, V. P. & Winklhofer, M. The osmotic magnetometer: a new model for a magnetite-based magnetoreceptor in animals. Eur. Biophys. J. 28, 380–392 (1999).
6. Leask, M. J. A physico-chemical mechanism for magnetic field detection by migratory birds and homing pigeons. Nature 267, 144–145 (1977).
7. Schulten, K. Magnetic field effects in chemistry and biology. Festkörperprobleme (Adv. Solid State Phys.) 22, 61–83 (1982).
8. Ritz, T., Adem, S. & Schulten, K. A photoreceptor-based model for magnetoreception in birds. Biophys. J. 78, 707–718 (2000).
9. Wiltschko, W., Munro, U., Ford, H. & Wiltschko, R. Red light disrupts magnetic orientation of migratory birds. Nature 364, 525–527 (1993).
10. Wiltschko, W. & Wiltschko, R. Magnetic compass orientation in birds and its physiological basis. Naturwissenschaften 89, 445–452 (2002).
11. Wiltschko, W., Traudt, J., Güntürkün, O., Prior, H. & Wiltschko, R. Lateralization of magnetic compass orientation in a migratory bird. Nature 419, 467–470 (2002).
12. Kobayashi, A. & Kirschvink, J. in Electromagnetic Fields: Biological Interactions and Mechanisms (ed. Blank, M.) 367–394 (American Chemical Society Books, Washington DC, 1995).
13. Weaver, J., Vaughn, T. & Astumian, R. Biological sensing of small differences by magnetically sensitive chemical reactions. Nature 405, 707–709 (2000).
14. Kirschvink, J. et al. in Sensory Transduction (eds Corey, D. & Roper, S.) 225–240 (Society of General Physiologists 45th Annu. Symp., Rockefeller Univ. Press, New York, 1992).
15. Cintolesi, F., Ritz, T., Kay, C., Timmel, C. & Hore, P. Anisotropic recombination of an immobilized photoinduced radical pair in a 50 µT magnetic field: a model avian photomagnetoreceptor. Chem. Phys. 294, 384–399 (2003).
16. Wiltschko, W. & Wiltschko, R. The effect of yellow and blue light on magnetic compass orientation in European Robins, Erithacus rubecula. J. Comp. Physiol. A 184, 295–299 (1999).
17. Wiltschko, W., Gesson, M. & Wiltschko, R. Magnetic compass orientation of European robins under 565 nm green light. Naturwissenschaften 88, 387–390 (2001).
18. Canfield, J., Belford, R., Debrunner, P. & Schulten, K. A perturbation theory treatment of oscillating magnetic fields in the radical pair mechanism. Chem. Phys. 182, 1–18 (1994).
19. Kirschvink, J. Microwave absorption by magnetite: a possible mechanism for coupling nonthermal levels of radiation to biological systems. Bioelectromagnetics 17, 187–194 (1996).
20. Beason, R. C. & Nichols, J. E. Magnetic orientation and magnetically sensitive material in a transequatorial migratory bird. Nature 309, 151–153 (1984).
21. Fleissner, G. et al. Ultrastructural analysis of a putative magnetoreceptor in the beak of homing pigeons. J. Comp. Neurol. 458, 350–360 (2003).
22. Beason, R. & Semm, P. Does the ophthalmic nerve carry magnetic navigational information? J. Exp. Biol. 199, 1241–1244 (1996).
23. Munro, U., Munro, J. A., Phillips, J. B., Wiltschko, R. & Wiltschko, W. Evidence for a magnetite-based navigational 'map' in birds. Naturwissenschaften 84, 26–28 (1997).
24. Wiltschko, W., Munro, U., Ford, H. & Wiltschko, R. Effect of a magnetic pulse on the orientation of silvereyes, Zosterops l. lateralis, during spring migration. J. Exp. Biol. 201, 3257–3261 (1998).
25. Semm, P. & Beason, R. C. Responses to small magnetic variations by the trigeminal system of the bobolink. Brain Res. Bull. 25, 735–740 (1990).
26. Beason, R. C. & Semm, P. in Acta XX Congr. Int. Ornithol. (ed. Bell, B. D.) 1813–1819 (New Zealand Ornithol. Congr. Trust Board, Wellington, 1991).
27. Batschelet, E. Circular Statistics in Biology (Academic, London, 1981).
28. Timmel, C., Cintolesi, F., Brocklehurst, B. & Hore, P. Model calculations of magnetic field effects on the recombination reactions of radicals with anisotropic hyperfine interactions. Chem. Phys. Lett. 334, 387–395 (2001).
29. Wiltschko, W. in Animal Migration, Navigation and Homing (eds Koenig, K. & Keeton, W.) 302–310 (Springer, Berlin, 1978).

Modelling disease outbreaks in realistic urban social networks

Stephen Eubank[1], **Hasan Guclu**[2], **V. S. Anil Kumar**[1], **Madhav V. Marathe**[1], **Aravind Srinivasan**[3], **Zoltán Toroczkai**[4] & **Nan Wang**[5]

[1]Basic and Applied Simulation Science Group, Los Alamos National Laboratory, MS M997, Los Alamos, New Mexico 87545, USA
[2]Department of Physics, Applied Physics and Astronomy, Rensselaer Polytechnic Institute 110 8th Street, Troy, New York 12180-3590, USA
[3]Department of Computer Science and Institute for Advanced Computer Studies, University of Maryland, College Park, Maryland 20742, USA
[4]Centre for Nonlinear Studies and Complex Systems Group, Los Alamos National Laboratory, MS B258, Los Alamos, New Mexico 87545, USA
[5]Department of Computer Science, University of Maryland, College Park, Maryland 20742, USA

Most mathematical models for the spread of disease use differential equations based on uniform mixing assumptions[1] or *ad hoc* models for the contact process[2–4]. Here we explore the use of dynamic bipartite graphs to model the physical contact patterns that result from movements of individuals between specific locations. The graphs are generated by large-scale individual-based urban traffic simulations built on actual census, land-use and population-mobility data. We find that the contact network among people is a strongly connected small-world-like[5] graph with a well-defined scale for the degree distribution. However, the locations graph is scale-free[6], which allows highly efficient outbreak detection by placing sensors in the hubs of the locations network. Within this large-scale simulation framework, we then analyse the relative merits of several proposed mitigation strategies for smallpox spread. Our results suggest that outbreaks can be contained by a strategy of targeted vaccination combined with early detection without resorting to mass vaccination of a population.

The dense social-contact networks characteristic of urban areas form a perfect fabric for fast, uncontrolled disease propagation. Current explosive trends in urbanization exacerbate the problem: it is estimated that by 2030 more than 60% of the world's population will live in cities[7]. This raises important questions, such as: How can an outbreak be contained before it becomes an epidemic, and what disease surveillance strategies should be implemented? Recent studies[1], under the assumption of homogeneous mixing, make the case for mass vaccination in response to a smallpox outbreak. With different assumptions, it has been shown[2] that mass vaccination is not required. Policymakers must trade off the risks associated with vaccinating a large population[8] against the poorly understood risks of losing control of an outbreak. Addressing such specific policy questions[9] requires a higher-resolution description of disease spread than that offered by the homogeneous-mixing assumption and the differential-equations approach.

Here we present a highly resolved agent-based simulation tool (EpiSims), which combines realistic estimates of population mobility, based on census and land-use data, with parameterized models for simulating the progress of a disease within a host and of transmission between hosts[10]. The simulation generates a large-scale, dynamic contact graph that replaces the differential equations of the classic approach. EpiSims is based on the Transportation Analysis and Simulation System (TRANSIMS) developed at Los Alamos National Laboratory, which produces estimates of social networks based on the assumption that the transportation infrastructure constrains people's choices about where and when to perform activities[11]. TRANSIMS creates a synthetic population endowed with demographics such as age and income, consistent with joint distributions in census data. It then estimates positions